Gold finger formation studied by high-resolution mass spectrometry and in silico methods

UNIVERSITÀ DEGLI STUDI DI TORINO

Gold finger formation studied by high-resolution mass spectrometry and *in silico* methods

Ü. A. Laskay,[a,‡] C. Garino,[b,‡] Y. O. Tsybin,[a] L. Salassa[c,d] and A. Casini[e,*]

[a] *Biomolecular Mass Spectrometry Laboratory, Ecole Polytechnique Fédérale de Lausanne (EPFL), 1015 Lausanne (Switzerland).*
[b] *Dept. of Chemistry and NIS Centre of Excellence, University of Turin, via Pietro Giuria 7, 10125 Turin (Italy).*
[c] *CIC biomaGUNE, Paseo de Miramón 182, 20009, Donostia–San Sebastián (Spain).*
[d] *Kimika Fakultatea, Euskal Herriko Unibertsitatea and Donostia International Physics Center (DIPC), P.K. 1072 Donostia, Euskadi (Spain).*
[e] *Dept. of Pharmacokinetics, Toxicology and Targeting, Research Institute of Pharmacy, Rijksuniversiteit Groningen, Antonius Deusinglaan 1, 9713AV Groningen (The Netherlands). Email: a.casini@rug.nl*

Abstract

High-resolution mass spectrometry and quantum mechanics/molecular mechanics studies were employed for characterizing the formation of two gold finger (GF) domains from the reaction of zinc fingers (ZF) with gold complexes. The influence of both the gold oxidation state and the ZF coordination sphere in GF formation provided useful insights into the possible design of new gold complexes targeting specific ZF motifs.

Zinc-finger (ZF) motifs belong to the *structural zinc* protein family where the zinc ion structurally organizes small peptidic domains (or bigger domains in case of multiple zinc ions) and the different coordination, interactions and arrangements can contribute to the structural and functional variety of these proteins.[1] ZFs were shown to be involved in a wide range of functions in DNA repairing, recognition, transcription, replication, apoptosis and metabolism. All of these processes are essential for cell growth and development, thus having direct implications in health and disease. Therefore, ZFs are frequently recognized as possible medicinal targets.

Metal-based compounds can affect ZF domain conformation either via zinc substitution or via oxidative damage, and therefore may be important in the development of new therapeutic drugs.[2] For example, several Pt and Co complexes have been shown to directly bind to transcription factors inhibiting their activities.[3] The antitumor drug cisplatin was found to be reactive towards ZF proteins, resulting in the ejection of zinc and the loss of secondary structure.[4, 5] Pl(II) and Au(III) complexes have been reported to interact with the C-terminal finger of the HIV nucleocapsid NCp7 ZF, leading to zinc displacement.[6] These latter studies show the opportunity of exploiting metallodrugs as a new class of anti-HIV agents based on inhibition of HIV NCp7 function. Recently, the same authors showed that a platinated single-stranded oligonucleotide can alter the structure of a model ZF peptide and characterized this interaction at a molecular level by NMR spectroscopy.[7] The ZF conformation change results from the formation of an adduct between the platinated oligonucleotide and the peptide, stabilized by strong H-bonding interactions.

Within this framework, some of us recently reported the inhibitory effects of different cytotoxic metal compounds including cisplatin, and a series of gold-based compounds with phosphine or bipyridyl ligands, towards the ZF enzyme poly(adenosine diphosphate (ADP)-ribose) polymerase 1 (PARP-1).[8, 9] Interestingly, Au(III) coordination complexes were among the most efficient in inhibiting purified PARP-1 followed by Au(I) compounds (IC_{50} in the nM or μM range, respectively). It is worth mentioning that PARPs play a key role in DNA repair by detecting DNA strand breaks and catalysing poly(ADP-ribosylation).[10] For this reason, PARPs have been referred to as ‘‘the guardian angels’’ of DNA, and are involved in cancer resistance to chemotherapies, including cisplatin-based ones.

Additional information on the reactivity of the metal complexes with PARP-1 N-terminal ZF domain was obtained by high-resolution mass spectrometry.[8] An excellent correlation between PARP-1 inhibition in protein extracts and the ability of the complexes to bind to the ZF motif (in competition with Zn^{2+}) was established. The results support a model whereby displacement of zinc from the PARP-1 ZF by gold ions leads to decreased PARP-1 activity, and to formation of the so-called “gold-finger” (GF).

Overall, these studies have shown that the extent and rate of zinc displacement by inorganic compounds in ZF domains can be modulated by the nature (metal, metal oxidation state, ligands) of the reacting compound. Nevertheless, an intrinsic issue in considering ZF as drug targets is that of specificity. Therefore, in order to achieve further insights into the reactivity of gold complexes at a molecular level, we decided to explore the binding of the Au(III) complex $[Au(phen)Cl_2]Cl$ (phen = 1,10-phenanthroline, Auphen) and of the Au(I) compound auranofin (Fig. 1) with a ZF having different zinc coordination sphere (Cys_2His_2), with respect to the one of PARP-1 ($Cys_2HisCys$).

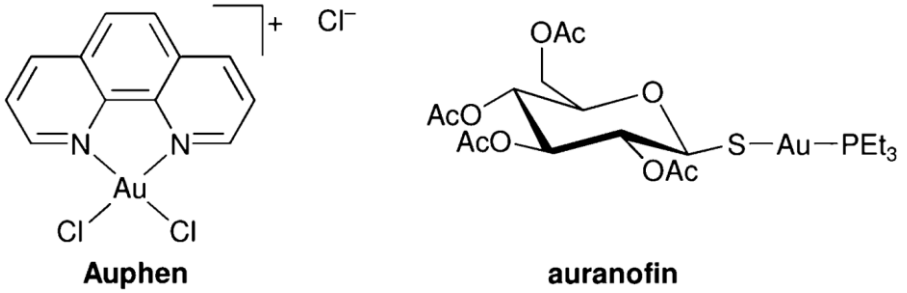

Auphen **auranofin**

Fig. 1 Gold complexes used in this study.

To assess whether coordination of the gold compounds to the zinc binding domain occurs via substitution of the Zn ion, with subsequent formation of GF, and to determine the binding stoichiometry, high-resolution electrospray ionization mass spectrometry (using the ESI Orbitrap FT-MS instrument) was applied.

In addition, a hybrid QM/MM (quantum mechanics/molecular mechanics) approach was used to determine the effects of binding of Au^{+} and Au^{3+} ions on the structure of model ZFs having either Cys_2His_2 or $Cys_2HisCys$ coordination motives, as well as possible selectivity patterns. In particular, the final aim of our computational study was to correlate the structural changes among ZF and GF domains with the loss in activity for biologically relevant targets containing ZF motifs such as PARP-1.

The MS analysis was carried out using the peptide PYK**C**PE**C**GKSFSQKSDLVK**H**QRT**H**TG (ZF2), initially in the absence of Zn^{2+} (apo-ZF2) with a complex-to-protein mole ratio of 3:1. Incubation of the complexes with the apo-ZF2 peptide (monoisotopic molecular mass $[M+H]^{+}$ 2961.4458 Da) leads to formation of new adducts. Fig. S1 and Fig. S2 in the ESI† show the broadband mass spectrum of the apo-ZF2 domain and of the ZF2-Auphen adduct, respectively. According to the results, Au is stripped of all ligands upon binding and the reaction is complete after 5 min incubation time. Only the non-reduced ZF2 is observed in the lower *m/z* region of the mass spectrum. Notably, the isotopic patterns analysis (ESI,† Fig. S2, inset) of a theoretical ZF2-Au(I) mono-adduct $(C_{127}H_{203}N_{39}O_{39}S_2Au(I))^{3+}$ matches the experimentally observed envelope of the highest intensity peak in the spectrum with a mass accuracy of 1.4 ppm. Conversely, the simulated pattern of the ZF2-Au(III) adduct $(C_{127}H_{201}N_{39}O_{39}S_2Au(III))^{3+}$ has a much lower monoisotopic mass (1052.4678 Da), and therefore, does not correspond to the Au charge state of the major product observed herein. However, a minor peak was observed at this lower mass, indicating that ~0.05% of the complex retains the metal as Au(III).

In the same conditions, the reaction of reduced ZF2 with auranofin is not complete, and a significant signal is recorded for the unreacted peptide (ESI,† Fig. S3). Moreover, the ratio of the unreacted and Au-bound ZF2 peaks is 1:1. Based on the simulated isotopic envelopes of the peptide containing Au(I) or Au(III), the oxidation state of the metal has been determined to be Au(I) and none of the original ligands have remained bound.

In general, in comparison to our previously reported data on apo-PARP-1 ZF where up to 3 Au^{+} ions could bind the peptide,[8] both complexes show a reduced reactivity with the ZF2 motif, and only Au mono-adducts could be detected.

In a second series of experiments the apo-ZF2 was incubated with zinc acetate in order to create the physiological ZF-motif. The zinc salt was added to the apo-ZF before the Au complexes to determine whether the metallodrugs are able to displace coordinated zinc (see ESI,† Experimental Section for details). Fig. S4 in the ESI† shows the broadband mass spectrum of the ZF2 peptide after 5 min incubation with Zn^{2+}. In the mass spectrum, no unbound peptide is observed and the major peak represents the ZF2-Zn adduct, corresponding to the peptide with elemental composition $(C_{127}H_{202}N_{39}O_{39}S_2Zn(II))^{3+}$. When Auphen was incubated with the ZF2-Zn complex in a 3:1 ratio, upon loss of the phen ligand, the oxidation state of gold was retained as Au(III) (Fig. 2), contrary to what was observed when the compound reacted directly with the apo-ZF. This reactivity is in accordance with our previous results on the PARP-1 ZF model where Auphen rapidly bound to the ZF domain, resulting in tetradentate binding of Au^{3+} ions through 1 His and 3 Cys residues (*vide infra*).

However, in the case of the ZF2-Zn peptide, in the time scale of the experiment (15 min incubation at r.t.) Au did not completely displace the Zn, and a significant signal for the ZF2-Zn complex was still visible in the mass spectrum at *m/z* 1009.13; the ratio of the ZF2-Zn and ZF2-Au(III) peaks being ~1.5. Notably, auranofin did not displace Zn from the ZF2-Zn complex at all, therefore no ZF2-Au peak was observed (data not shown).

The obtained MS data are summarized in Table 1 compared to our previous results on PARP-1 ZF domain[8]. Interestingly, the results on the interaction of auranofin with the apo-ZF2 peptide are supported by those previously reported by Barrios *et al*., who studied the interactions of $[Au(PEt_3)Cl_2]$ with the same zinc finger

model (ZF2).[11] In this latter case, evidence for Au(I) binding to apo-ZF2 was inferred by the distortion of the peptide secondary structure observed by Circular Dichroism.

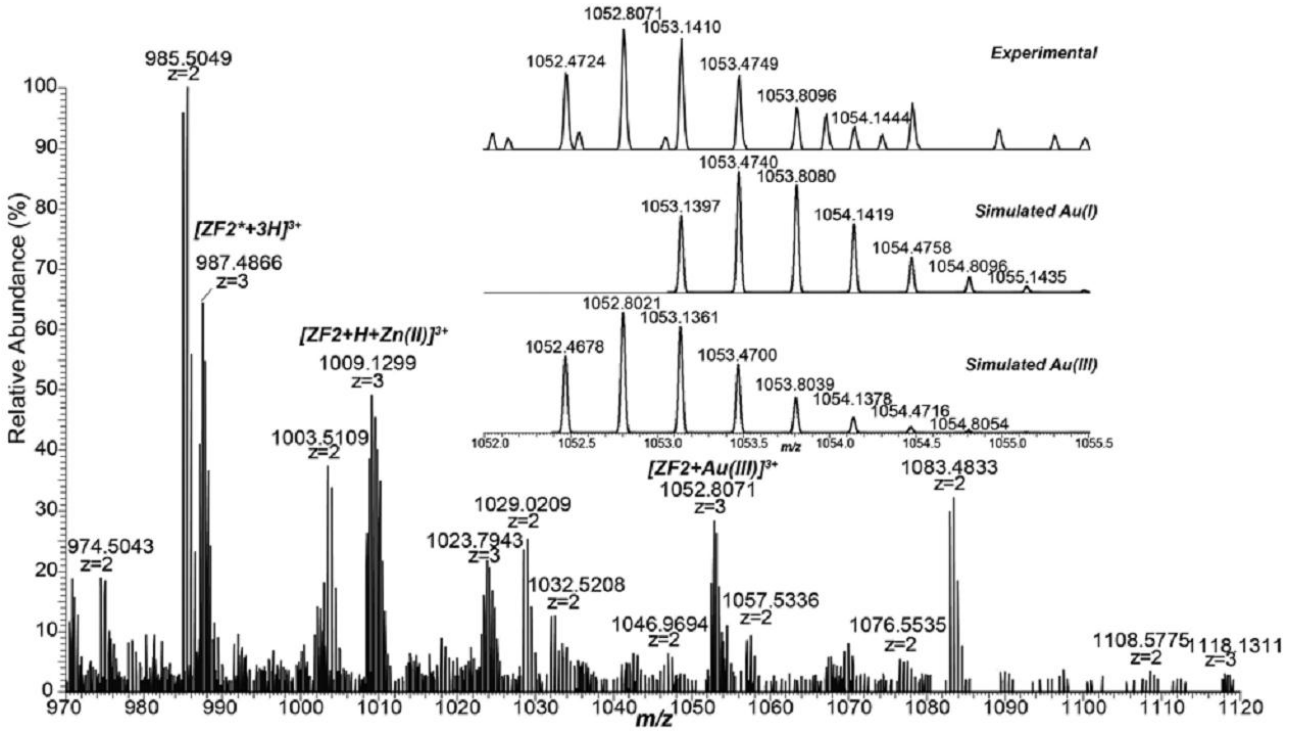

Fig. 2 ESI Orbitrap FT MS mass spectrumof the ZF2–Auphen adduct recorded after 5 min incubation with Zn^{2+} followed by 15 min incubation with Auphen. The insets compare the experimental isotopic pattern of peptide–metal complex with the simulated isotopic patterns of the $(C_{127}H_{203}N_{39}O_{39}S_2Au(I))^{3+}$ and $(C_{127}H_{201}N_{39}O_{39}S_2Au(III))^{3+}$ composition peptides.

Table 1 Summary of the gold-bound species arising from the reactivity of gold compounds with different zinc finger domains as detected by MS

	Cys_2His_2		$Cys_2HisCys$	
Compound	apo-ZF2	Zn-ZF2	apo-PARP1	Zn-PARP1
Auphen	Au(I) monoadduct	Au(III) monoadduct	Up to 3 Au atoms: two Au(III) amd one Au(I)	Au(III) monoadduct
auranofin	Au(I) monoadduct	No monoadduct	Up to 2 Au(I) atoms	Au(I) monoadduct

A goal of our *in silico* study was the identification of potential selective interactions of gold complexes with different ZF coordination spheres, and to explain the observed differences in reactivity evidenced by MS. Thus, the Cys_2His_2 Xfin-31 ZF NMR structure (**1**), corresponding to the 31st ZF from the Xenopus protein Xfin, was employed as a starting point and reference to perform QM/MM calculations (ONIOM method) aimed at characterizing the geometry of a series of ZFs motives coordinating Zn^{2+} in Cys_2His_2 (**2a**) and $Cys_2HisCys$ (**2b**) environments. Afterwards, the geometry of the corresponding GFs, binding either Au^+ (**3a** and **3b**) or Au^{3+} (**4a** and **4b**) ions, were also determined (Fig. 3 and ESI,† Table S1). The choice of the peptide was based on both the similarity with the ZF model structure used in the MS work (74% structural overlap§), and on the availability of the corresponding NMR structure.

Details on the computational approach are reported in the experimental section of the ESI†. Briefly, the ONIOM[12-14] QM/MM method as implemented in Gaussian 09[15] was employed at the level QM@B3LYP/SDD/6-31G*[16-18] and MM@Amber/ff9[19-21] using the package TAO[22] for preparation of input files and data analysis. The Au AMBER parameters required for running the MM part were obtained from QM calculation on small molecular models, namely $[Au(Cys)_2(His)_2]^{-/+}$ and $[Au(Cys)_3(His)]^{2-/0}$ (ESI,† Fig. S5 and Table S2).

As shown in Fig. S6 of the ESI,† the calculated structure **2a** well matches the experimental one obtained by NMR (**1**). The Zn^{2+} ion folds together the two major structural units of the small protein, the β-sheet which contains two Cys residues and the α-helix containing two His. Substitution of His23 for Cys23 (to achieve a $Cys_2HisCys$ domain) does not affect significantly the overall structure of the ZF as shown by the close similarity of **2a** and **2b** in Fig. 3. The resemblance between the two peptides is due to rather unperturbed Zn coordination sphere which only displays small differences between the Zn–N_τ(His23) and Zn–S(Cys23) distances, 2.167 Å and 2.482 Å, for **2a** and **2b**, respectively. The tetrahedral coordination of the Zn^{2+} is fundamental to maintain the secondary structure of both the N- and C-terminus domains, hence the tertiary structure of the whole ZF model.

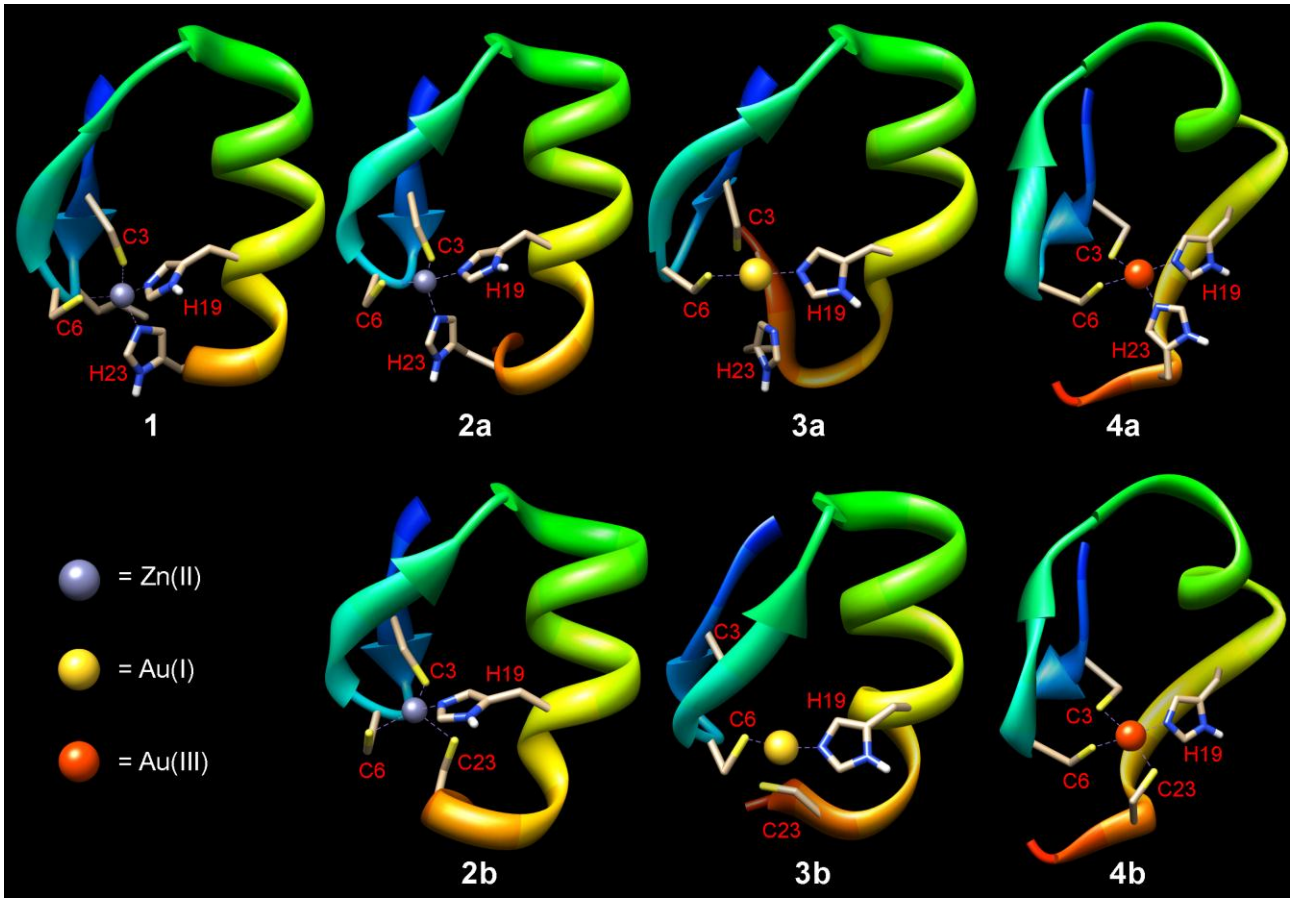

Fig. 3 NMR structure (**1**) of the 31st zinc finger from the Xenopus protein Xfin (Xfin-31, pdb code 1ZNF) compared to the optimized QM/MM structures obtained from the Xfin31 Cys_2His_2 peptide (**2a**–**4a**) and its $Cys_2HisCys$ analogue (**2b**–**4b**). Coordination sphere a = Cys_2His_2, b = $Cys_2HisCys$.

When Zn^{2+} is replaced by a Au^+ ion and the geometry of the GF is optimized (**3a** and **3b**, Fig. 3), the metal centre only coordinates two of the four amino acids, His19 and Cys6, involved in the ZFs. The outcome is consistent with the typical linear coordination geometry of Au(I). Such behaviour is also observed in the case of the small molecular models (ESI,† Fig. S5).

Interestingly, in spite of the dramatic change in the coordination environment around the metal centre, the overall structure of the peptide is only partially affected. The two units are still kept in close proximity by the coordinating His19 and Cys6 residues and by other Van der Waals weak interactions. In 3a, the β-sheet containing the terminal NH_2 group displays an H-bond (N–H···S, 2.042 Å) between the Cys13 and the Gln20 residues, which contributes to the GF folding. An H-bond interaction (2.259 Å) is also present between Gln20 and Cys23 in 3b, contributing to the preservation of the α-helix (ESI,† Fig. S7).

In general, it can be concluded that **3a** and **3b** have structural features closely resembling **2a** and **2b**, respectively, with the Cys_2His_2 structures being more alike each other (Fig. 4A for **2a** and **3a**). Only the terminal ends of the GFs appear slightly different as a result of the reduced metal coordination. It is also

worth mentioning that weak Van der Waals contacts are present between the Au(I) and the uncoordinated His23 (3.733 Å) and the Cys3 (4.669 Å) in **3a** and **3b** respectively (ESI,† Fig. S7). Taking into account the known high affinity of Au^{+} ions to sulphur donors and accordingly with previously reported results,[23] the structure of an analogue of **3a**, where the Au^{+} ion is coordinated by two Cys (Cys3 and Cys6) was also optimized (**3c**, ESI,† Fig. S8). No marked structural differences with **2a** and **3a** are present, except for a shift in the position of the metal (ESI,† Fig. S9 and Fig. S10). However, it is realistic to expect a (partial) loss in the tertiary structure of **3c** due to the lack of interaction between the α-helix and the Au(I) centre.

The structures of two Au(I)-GFs bearing a protonated Cys23 (**5a** and **5b**, ESI,† Fig. S11) were also calculated for comparison purposes and for interpretation of experimental data, since mass spectrometry results published earlier indicated that protonation of Cys residue could occur in Au(I)-GFs.[8] In comparison with their deprotonated analogues (**3a** and **3b**), these structures show more pronounced distortions with respect to the Zn-containing **2a** and **2b**.

Remarkably, when Au^{3+} was introduced in the ZF domain, more relevant conformational changes were observed. An overlay between the ZFs and the Au(III)-GFs is reported in Fig. 4B (**2a** and **4a**) and in ESI,† Fig. S12 (**2b** and **4b**). It can be noted that the optimized structures **4a** and **4b**, bearing a Au(III) metal centre, are markedly more distorted with respect to their ZF and Au(I)-GF analogues, with the most dramatic effect being the unfolding of the α-helix. Distortion of the β-sheet structure is also occurring. The overall unfolding of these GF structures is particularly evident in the hydrophobicity surface plotting (Fig. 4C). This result is in good accordance with previously reported circular dichroism studies on the reactivity of Au(III) complexes with similar ZF models,[6] and can be rationalized taking into account that, although Au(III) is four coordinated as Zn(II), it favours a square planar coordination sphere over a tetrahedral geometry, causing major changes in the peptide structure. Such a distortion ultimately could result in the loss of GF activity and marked inhibition of the entire protein function, as in the case of the PARP-1 enzyme.

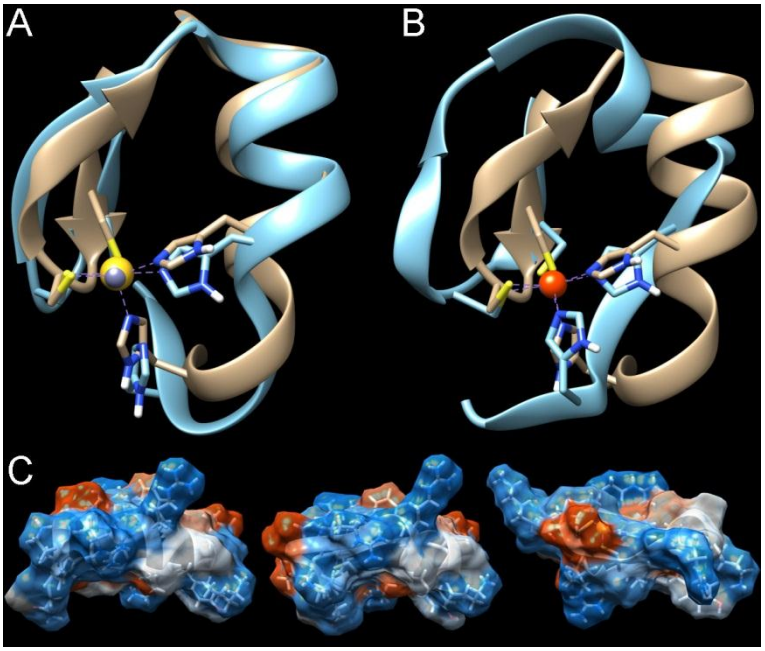

Fig. 4 (A) Overlap between the calculated structures of **2a** (brown) and **3a** (blue). (B) Overlap between the calculated structures of **2a** (brown) and **4a** (blue). (C) Hydrophobicity surfaces of **2a** (left), **3a** (middle) and **4a** (right)

In conclusion, we report here on the study of the interactions of gold complexes with ZF domains. High-resolution ESI Orbitrap FT-MS showed that both Au(I) and Au(III) are able to efficiently bind to ZF domains displacing the native Zn^{2+} ion. Moreover, the Au(III) compound Auphen is more effective than the Au(I) compound auranofin in replacing zinc from the ZF2 peptide. Interestingly, both complexes are less reactive with this model peptide than with the PARP-1 ZF model used in previous studies.[8] Most importantly, auranofin showed marked selectivity for the $Cys_2HisCys$ motif (Table 1), indicating that Au(I) complexes may be more suitable to target this type of ZF domain (i.e. to design selective PARP-1 inhibitors).

Overall, the results suggest the influence of different zinc coordination spheres (Cys_2His_2 *vs* $Cys_2HisCys$) in the formation of GFs, with the domain of PARP-1 richer in Cys residues being the most reactive. Our results are in line with previously reported ones by Farrell *et al.* pointing at the contribution of the nature of the ZF domain in the modulation of Au(I) compounds biological activity,[23] although in this latter case, the investigated compounds belonged to the family of the Au(I) phosphine-N-heterocycles.

Moreover, in our model peptides, both the Cys_2His_2 and $Cys_2HisCys$ cores favour the maintenance of the Au(III) oxidation state upon binding, while incubation of the corresponding apo-ZF domains with Auphen leads to reduction to Au(I).

As evidenced by our QM/MM calculations, and in accordance with the previously reported PARP-1 inhibition studies, Au(III) compounds are likely to inhibit ZF activity better than Au(I) probably due to a larger distortion of the peptide structure upon GF formation. Nevertheless, Auphen showed scarce selectivity with respect to the type of ZF domain (Table 1), which may favour off-target effects.

Determining the structural changes induced by the substitution of Zn^{2+} with Au ions in ZFs and to correlate them to possible inhibition properties is fundamental to the understanding of the mechanism of action of Au-based cytotoxic agents at a molecular level. In fact, ZF enzymes may constitute realistic pharmacological targets for this promising class of metal compounds. In this respect, it is worth mentioning that both Auphen and auranofin possess anticancer properties *in vitro*.[24, 25] Most importantly, our initial data support the design of gold-based electrophilic agents for inactivation of selected ZF medicinal targets.

Acknowledgements

A. C. thanks the University of Groningen (Rosalind Franklin Fellowship) for financial support. We thank Kristina Srzentić for the assistance with sample preparation and MS analysis. L.S. is supported by the MICINN of Spain with the Ramón y Cajal Fellowship RYC-2011-07787. The SGI/IZO-SGIker UPV/EHU is gratefully acknowledged for generous allocation of computational resources. L.S. is also grateful to Prof. J. M. Ugalde, Dr. T. Mercero and Dr. E. Ogando for their support. Members of the European COST Action CM1105 are gratefully acknowledged for stimulating discussions.

Notes and references

† Electronic supplementary information (ESI) available: Experimental section, Fig. S1–S9 and Table S1. See DOI: 10.1039/c4cc07490d

‡ These two authors contributed equally to the work.

§ Obtained using the Lalign sequence alignment software from the FASTA package.

1. J. A. Tainer, M. M. Thayer and R. P. Cunningham, *Cur. Opin. Struct. Biol.*, 1995, **5**, 20-26.
2. A. Witkiewicz-Kucharczyk and W. Bal, *Toxicol. Lett.*, 2006, **162**, 29-42.
3. C. H. Leung, H. Z. He, L. J. Liu, M. D. Wang, D. S. H. Chan and D. L. Ma, *Coord. Chem. Rev.*, 2013, **257**, 3139-3151.
4. R. N. Bose, W. W. Yang and F. Evanics, *Inorg. Chim. Acta*, 2005, **358**, 2844-2854.
5. L. Maurmann and R. N. Bose, *Dalton Trans.*, 2010, **39**, 7968-7979.
6. Q. A. de Paula, J. B. Mangrum and N. P. Farrell, *J. Inorg. Biochem.*, 2009, **103**, 1347-1354.
7. S. Quintal, A. Viegas, S. Erhardt, E. J. Cabrita and N. P. Farrell, *Biochem.*, 2012, **51**, 1752-1761.
8. F. Mendes, M. Groessl, A. A. Nazarov, Y. O. Tsybin, G. Sava, I. Santos, P. J. Dyson and A. Casini, *J. Med. Chem.*, 2011, **54**, 2196-2206.
9. M. Serratrice, F. Edafe, F. Mendes, R. Scopelliti, S. M. Zakeeruddin, M. Gratzel, I. Santos, M. A. Cinellu and A. Casini, *Dalton Trans.*, 2012, **41**, 3287-3293.
10. V. Schreiber, F. Dantzer, J. C. Ame and G. de Murcia, *Nat. Rev. Mol. Cell Biol.*, 2006, **7**, 517-528.
11. M. A. Franzman and A. M. Barrios, *Inorg. Chem.*, 2008, **47**, 3928-3930.
12. S. Dapprich, I. Komaromi, K. S. Byun, K. Morokuma and M. J. Frisch, *Theochem-J. Mol. Struct.*, 1999, **461**, 1-21.
13. M. Svensson, S. Humbel, R. D. J. Froese, T. Matsubara, S. Sieber and K. Morokuma, *J. Phys. Chem.*, 1996, **100**, 19357-19363.
14. T. Vreven, K. S. Byun, I. Komaromi, S. Dapprich, J. A. Montgomery, K. Morokuma and M. J. Frisch, *J. Chem. Theory Comput.*, 2006, **2**, 815-826.

15. M. J. Frisch et al., Gaussian 09 revision B.01, Gaussian Inc., Wallingford CT, 2009.
16. A. D. Becke, *J. Chem. Phys.*, 1993, **98**, 5648-5652.
17. P. Fuentealba, H. Preuss, H. Stoll and L. Vonszentpaly, *Chem. Phys. Lett.*, 1982, **89**, 418-422.
18. A. D. Mclean and G. S. Chandler, *J. Chem. Phys.*, 1980, **72**, 5639-5648.
19. W. D. Cornell, P. Cieplak, C. I. Bayly, I. R. Gould, K. M. Merz, D. M. Ferguson, D. C. Spellmeyer, T. Fox, J. W. Caldwell and P. A. Kollman, *J. Am. Chem. Soc.*, 1995, **117**, 5179-5197.
20. M. B. Peters, Y. Yang, B. Wang, L. Fusti-Molnar, M. N. Weaver and K. M. Merz, *J. Chem. Theory Comput.*, 2010, **6**, 2935-2947.
21. J. M. Wang, P. Cieplak and P. A. Kollman, *J. Comput. Chem.*, 2000, **21**, 1049-1074.
22. P. Tao and H. B. Schlegel, *J. Comput. Chem.*, 2010, **31**, 2363-2369.
23. C. Abbehausen, E. J. Peterson, R. E. F. de Paiva, P. P. Corbi, A. L. B. Formiga, Y. Qu and N. P. Farrell, *Inorg. Chem.*, 2013, **52**, 11280-11287.
24. M. Coronnello, G. Marcon, S. Carotti, B. Caciagli, E. Mini, T. Mazzei, P. Orioli and L. Messori, *Oncol. Res.*, 2000, **12**, 361-370.
25. S. Nobili, E. Mini, I. Landini, C. Gabbiani, A. Casini and L. Messori, *Med. Res. Rev.*, 2010, **30**, 550-580.